Simulation of Methane Adsorption in ANG Storage System

P.K. Sahoo[1], K.G. Ayappa[*,1] , M. John[2] , B.L. Newalkar[2] and N.V. Choudary[2]

[1]Department of Chemical Engineering, Indian Institute of Science, Bangalore- 560 012

[2]Corporate R&D Centre, Bharat Petroleum Corporation Ltd.,Greater Noida

*Corresponding author: Department of Chemical Engineering, Indian Institute of Science, Bangalore- 560012, E-mail : ayappa@chemeng.iisc.ernet.in

Abstract: Recently adsorptive storage has been identified as the most promising low-pressure (3.5 - 4.0 MPa) alternative for storing natural gas for vehicular use. However in order to successfully implement this technology, the filling and discharge characteristics of the adsorbent bed must be well understood. Significant temperature changes that occur during adsorption and desorption retard the system performance. In this work thermal effects associated with dynamic charge of methane in a 1.82 *l* adsorbed natural gas (ANG) cylinder filled with activated carbon, has been studied both theoretically and experimentally. A finite element simulation (COMSOL MULTIPHYSICS) of such a natural gas storage cylinder, based on a 2D model where hydrodynamics, heat transfer and adsorption phenomena are coupled, is presented. The transient temperature profiles in the adsorbent bed are obtained during the charging process through the simulation. The experimental study has been carried out in a packed bed of granular activated carbon (Norit-RGM1) at various charging rates to measure temperatures at various positions in the bed. The temperature profiles obtained from experiments are in good agreement with the model prediction. Although a higher charging rate of methane reduces filling time, a large bed temperature rise retards the storage capacity of the ANG cylinder.

Keywords: Methane, Adsorption, ANG, Activated Carbon, Thermal effects, Finite element method

1. Introduction

The abundant reserve of natural gas on earth has been recognized as an alternative fuel for the transportation sector. A relatively clean-burning quality and high octane number compared to that of gasoline, makes it attractive for vehicular use. Unfortunately, a much lower storage density of methane (the major constituent of natural gas) compared to that of conventional liquid fuels makes it inconvenient for onboard storage and transportation.

In order to enhance the storage density of methane, attention has been focused worldwide on the development of adsorbed natural gas (ANG) systems. In the ANG system, natural gas is stored as an adsorbed state in porous adsorbents at a pressure of (3.5 MPa – 4 MPa). The storage target of 180 V/V (i.e. liters of gas stored per liter of storage vessel internal volume under STP conditions) for ANG is yet to be achieved at a commercial level. A successful ANG system depends not only on appropriate adsorbents, but also on proper thermal management during the adsorption/desorption process [1]. The release of significant heat during adsorption and cooling during desorption, has detrimental effects on the performance of the storage system. As a result a lower amount of gas is stored at the target pressure during the charging cycle and a residual amount of stored gas is retained in the cylinder at the depletion pressure during the discharge cycle [4]. The variations in adsorbent bed temperature during fast/slow filling/discharge of gas are available in the literature [2, 3, 6, 8] on a wide variety of adsorbents. In order to optimize between filling times and storage capacity of the ANG system, the main objective of this work is to simulate the thermal effects during dynamic charging of methane gas at controlled rate in the packed bed of adsorbent.

2. Description of ANG Storage System

A 1.82 *l* prototype cylindrical ANG storage system as used in this study is depicted in Fig. 1

with dimensions. It consists of a small opening of radius (r_i) of 3.175 mm at the top for charging of methane gas (99.9% purity used in experiments) to the storage system. It is filled and packed densely with a commercially available adsorbent (i.e. Norit RGM1 activated carbon having average particle diameter of 1.0 mm and bulk density of 0.5 g cc^{-1}) by automated tapping. A controlled methane flow rate during charging process has been maintained by a mass flow controller (Bronkhorst type) with flows in the range of 1–50 *l* min^{-1} at NTP. A pressure gauge is provided at the inlet of the cylinder for monitoring the pressure during charging. A K-type thermocouple is provided at the centre of bed both axially and radially for measurement of temperature. During charging, the pressure and temperatures of the adsorbent bed have been recorded at regular intervals of time until cylinder pressure reaches 3.5 MPa.

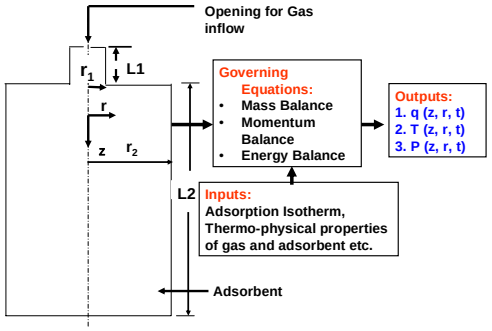

Figure 1. Schematic diagram of the ANG storage system with dimensions: r_1 = 13 mm, r_2 = 53.3 mm, L1= 30 mm and L2 = 202 mm.

As shown in Fig. 1 a two dimensional axi-symmetric model is assumed for transient heat transfer analysis of the problem. The thermo-physical properties of Norit-RGM1 carbon, methane and other relevant data used in the simulation are shown in Table 1.

3. Model Development

3.1 Governing Equations

The assumptions in the model are as follows:
(i) Methane behaves an ideal gas. The gas properties are constant in the range of temperatures and pressures.
(ii) All thermo-physical properties (density, specific heat, thermal conductivity etc.) of the adsorbent bed are constant in the range of temperatures and pressures under consideration.
(iii) The adsorbed gas phase and solids are locally in thermal equilibrium with the gas phase.
(iv) Intraparticle and film resistances to mass and heat transfer are neglected.
(v) Natural convection inside the packed bed is neglected.
(vi) The heat of adsorption is constant.
(vii) The thermal effect of the ANG cylinder wall is neglected.

Table 1 Data used in simulation

C_{pg} =2450 J kg^{-1} K^{-1}	C_{ps} = 650 J kg^{-1} K^{-1}
ΔH = 16 kJ mol^{-1}	M_g =16.03 x10^{-3} kg mol^{-1}
T_i= 303 K	T_{ext} = 303 K
T_s = 303 K	ε_{eff} = 0.65
λ_g = 0.0343 $Wm^{-1}K^{-1}$	λ_s = 0.50 $Wm^{-1}K^{-1}$
μ_g = 1.25 x 10^{-5} Pa.s	ρ_b = 500 kg m^{-3}

The model consists of the following governing equations.

3.1.1 Continuity Equation

$$\frac{\partial}{\partial t}\left(\varepsilon_t \rho_g + \rho_b q\right) + \nabla\cdot\left(\rho_g \mathbf{u_g}\right) = 0 \qquad (1)$$

where $\varepsilon_t = \varepsilon_b + (1-\varepsilon_b)\varepsilon_p$ is the porosity accessible to the gas phase and ε_b and ε_p are porosities of adsorbent bed and adsorbent particles respectively. ρ_b is the packing density of bed. q is the adsorbed gas concentration, which is defined as the kg of gas adsorbed per kg of adsorbent and $\mathbf{u_g}$ is gas velocity.

From ideal gas law, $\rho_g = \frac{PM_g}{RT}$, where, M_g is the molecular weight of gas and R is the Universal gas constant, P and T are pressure and temperature of the gas respectively.

3.1.2 Momentum Equation

$$\frac{\rho_g}{\varepsilon_t}\frac{\partial \mathbf{u_g}}{\partial t} + \frac{\rho_g}{\varepsilon_t^2}\left(\mathbf{u_g}\cdot\nabla\right)\mathbf{u_g} = -\nabla P + \mu_g \nabla^2 \mathbf{u_g} - \frac{\mu_g}{K}\mathbf{u_g} \qquad (2)$$

where μ_g is the gas viscosity and the permeability of the bed $K = \frac{4\varepsilon_b^3 R_p^2}{150(1-\varepsilon_b)^2}$

where, R_p is the adsorbent particle radius.

3.1.3 Energy Equation

$$\rho C_p \frac{\partial T}{\partial t} + C_{pg}\nabla\cdot\left(T\rho_g \mathbf{u_g}\right) = \nabla\cdot\left(\lambda_{eff}\nabla T\right) + \rho_b|\Delta H|\frac{\partial q}{\partial t} + \varepsilon_t R\rho_g \frac{\partial T}{\partial t} \quad (3)$$

where,

$\rho C_p = \left(\varepsilon_t\rho_g + \rho_b q\right)C_{pg} + \left(1-\varepsilon_t\right)\rho_s C_{ps}$,

$\rho_b = \left(1-\varepsilon_t\right)\rho_s$ and ρ_s is the density of carbon particles, C_{ps} and C_{pg} are specific heats of adsorbent and gas respectively. The effective thermal conductivity (λ_{eff}) of the bed is $\lambda_{eff} = \varepsilon_t\lambda_g + \left(1-\varepsilon_t\right)\lambda_s$ where, λ_g and λ_s are thermal conductivities of gas and carbon respectively. ΔH is the isosteric heat of adsorption.

3.1.4 Scheme for Methane Adsorption

Amount of gas adsorbed (q) is calculated by the well known Dubinin-Astakhov (DA) equation as:

$$q = \rho_{ads} W_o \exp\left[-\left(\frac{A}{\beta E_o}\right)^n\right] \quad (4)$$

where, ρ_{ads} is the adsorbed gas density, W_o is the microporous volume per kg of adsorbent, β is the affinity coefficient related to adsorbate-adsorbent interaction, the value of which is 0.35 for methane adsorption [7]. E_o is the characteristic energy of adsorption and n is the DA exponent related to the pore size dispersion. After fitting our experimental isotherm data of Norit RGM1 sample at temperature of 303K to DA equation, the relevant DA parameters are E_o = 28571.43 J mol^{-1}, W_o= 0.0003108 m^3 kg^{-1} and n=2.0 have been estimated.

The Polany adsorption potential $A = RT\ln\left(\frac{P_s}{P}\right)$, where the saturated vapour pressure of the gas (P_s) is calculated using the Dubinin form as $P_s = P_{cr}\left(\frac{T}{T_{cr}}\right)^2$ where, P_{cr} and T_{cr} are critical pressure and critical temperature of gas respectively.

The adsorbed gas density (ρ_{ads}) is expressed by Osawa et al. [5] as $\rho_{ads} = \frac{\overline{\rho}_{ads}}{\exp\left[\alpha_e\left(T - \overline{T}_b\right)\right]}$ where, $\overline{\rho}_{ads}$ is the density of liquid methane at boiling point ($\overline{T}_b$) and α_e is the mean value of thermal expansion of liquefied gases.

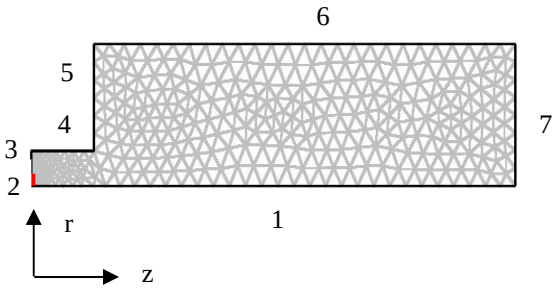

Figure 2. 2D axi-symmetric geometry used for simulation, with the inlet of radius r_i depicted as 2

3.2 Initial Conditions

For, $t = 0$, r, z $\in \Omega$, where Ω is the domain as illustrated in Fig. 2.

$P(z, r) = P_i = 0.1$ MPa (5)

$T(z, r) = T_i = 300$K/ 308 K (6)

$q = q(P_i, T_i)$ (7)

where, P_i and T_i are initial pressure and temperature in adsorbent bed. T_i has been taken 300 K and 308 K at the time of charging the cylinder at 1.0 *l* min^{-1} and 30.0 *l* min^{-1} respectively based on the ambient temperature conditions.

3.3 Boundary Conditions

At the opening for gas inlet (boundary 2 as shown in Fig. 2), the following boundary condition is applied:

For $z = 0$ and $0 \le r \le r_i$

$u_g = u_{inlet}$ (8)

u_g of gas is calculated from the charging, the density at the charging condition and cross sectional area of the inlet.

Heat flux inlet boundary condition for adsorption is shown as

$$C_{pg}\left(T_s - T\right)\rho_g u_{inlet} = -\lambda_{eff}\frac{\partial T}{\partial z} \quad (9)$$

T_s and T_{ext} are gas source and external ambient temperatures respectively.

The symmetry boundary condition has been taken along the axis (i.e. boundary 1). Wall with no slip boundary condition is taken at boundaries 3,4,5,6 and 7 for flow equations. The convective heat flux boundary condition has been taken in boundaries 3, 4, 5, 6 and 7 for energy equation as

$$-\lambda_{eff}\nabla T = h_c\left(T_{ext} - T\right) \quad (10)$$

where, h_c is the convective heat transfer coefficient to ambient air on the adsorbent bed surface.

Equation system (1)-(4) defines four variables P, T, q and $\mathbf{u_g}$ dependent from space co-ordinates and time. The differential equations are solved using the COMSOL MULTIPHYSICS 3.5a software, which is based on the finite element method and the triangular mesh used is illustrated in Fig. 2. Convergence criterion is 10^{-6}.

4. Results and Discussion

From Figures 3 and 4 it is quite evident that the temperature predicted by the model is in good agreement with the experimental results. It is seen that the temperature at the centre of bed increases with time and reaches its maximum towards the end of filling. At a charging rate of 1.0 *l* min^{-1}, a maximum temperature increase of 21^0 (Fig. 3) is obtained at the centre of the bed, whereas for fast charging of 30.0 *l* min^{-1}, the maximum temperature increase of about 58^0 (Fig. 4) is obtained. Earlier Goetz and Biloé [3] have reported the maximum temperature increase of 47^0 at charging rate of 7.5 *l* min^{-1} at the centre of storage cylinder with adsorbent composite blocks (ACB) made from activated carbon Maxsorb with binder of expanded natural graphite. Maximum temperature at the centre of the adsorbent bed is observed since it is located at the largest distance from the surrounding environment, with which heat exchange takes place.

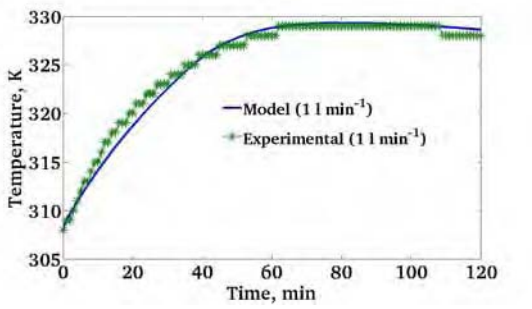

Figure 3. Temperature changes at the centre of bed with time during charging of ANG cylinder at fixed flow rate of 1.0 *l* min^{-1}

The surface temperature profiles of adsorbent bed with various time intervals during a slow charging rate at 1.0 *l* min^{-1} and fast charging rate at 30.0 *l* min^{-1} have been depicted in Figs. 5 and 6 respectively. In an adsorption cycle, adsorption usually starts from the inlet and the adsorption front moves towards the interior of the bed in both axial and radial directions with flow of gas. With progress of time, shifting of the adsorption front from inlet towards the interior of the cylinder is indicated by the increased temperatures on the surface of adsorbent bed. During a charging process, the adsorption phenomena inside the cylinder takes place under such conditions, where the adsorbent bed gets enough time to exchange heat through its outer wall with the surrounding ambient environment. For these reason a maximum temperature of 329 K is developed at the centre of the bed after 120 min of charging the cylinder at 1.0 *l* min^{-1} as shown in Fig. 5(c). However a fast charging of gas at 30.0 *l* min^{-1} approaches to an adiabatic process inside the storage cylinder so that the adsorbent bed does not get enough time to exchange heat with the surrounding environment. As a consequence the bed temperature rises quickly as observed from the temperature maps in Fig. 6.

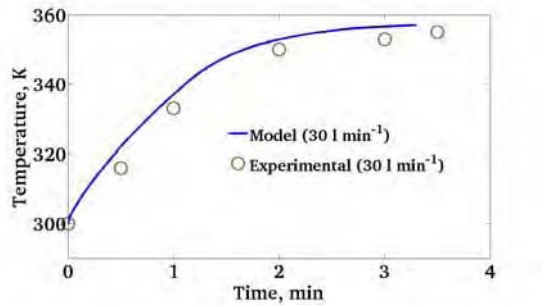

Figure 4. Temperature changes at the centre of bed with time during charging of ANG cylinder at fixed flow rate of 30.0 *l* min^{-1}

As per the ideal gas law the increase of temperature in the adsorbent bed retards the storage capacity. Filling time (t_f), filling capacity (V_f) and maximum temperature increase (ΔT_{max}) of storage cylinder for different charging rates of methane have been listed in Table 2. Filling time (t_f) is the time at which the ANG cylinder attains 3.5 MPa pressure during charging operation. Filling capacity (V_f) is the volume of gas in litres filled into the ANG cylinder at the end of the filling time (t_f). Usually filling capacity of ANG cylinder is expressed as V/V basis, which is the ratio of V_f to the volume of adsorbent bed (V_b). The V/V basis filling capacity of the ANG cylinder at different charging rates are presented in Table 2. Maximum temperature increase (ΔT_{max}) in the storage cylinder is the difference between the maximum temperature (that occurs at the centre of bed as depicted in Figs. 5 and 6) and the initial temperature in the bed. Storage capacity of cylinder reduces by 17.5% when charging rate is increased from 1.0 *l* min^{-1} to 30.0 *l* min^{-1}. The long filling time of 120 minutes at

1.0 *l* min^{-1} charging rate makes the system impractical. On the other hand practically feasible filling time of about 3.3 minutes at 30.0 *l* min^{-1} charging rate also makes the system inefficient due to significant reduction in storage capacity of about 17.5%.

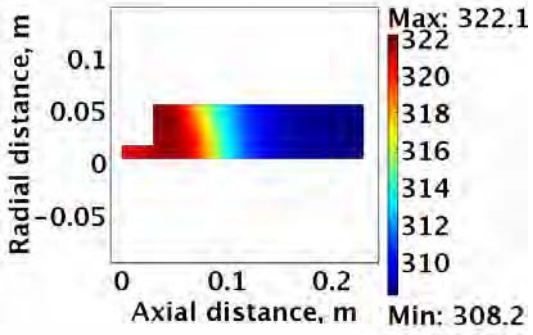

(a) 5 min

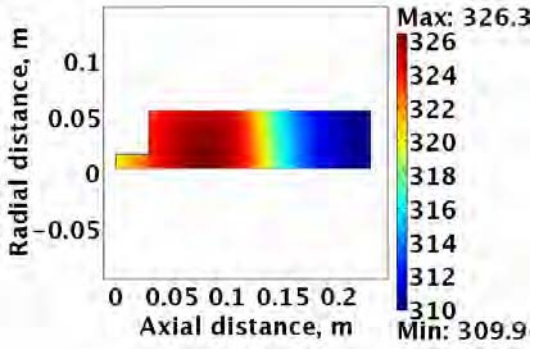

(b) 30 min

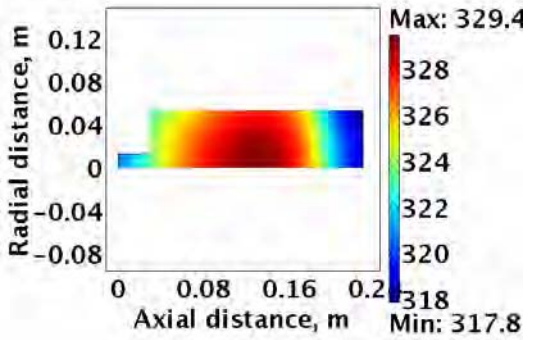

(c) 120 min

Figure 5. Temperature maps in the adsorbent bed at different times during charging of ANG cylinder at a flow rate of 1.0 *l* min^{-1}.

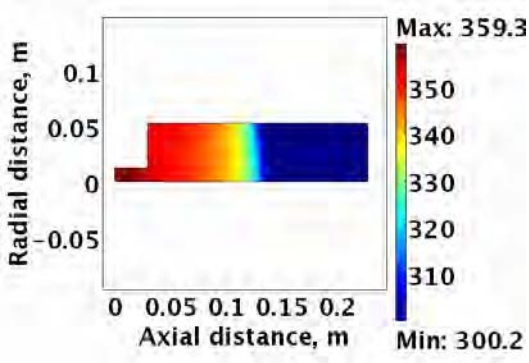

(a) 1 min

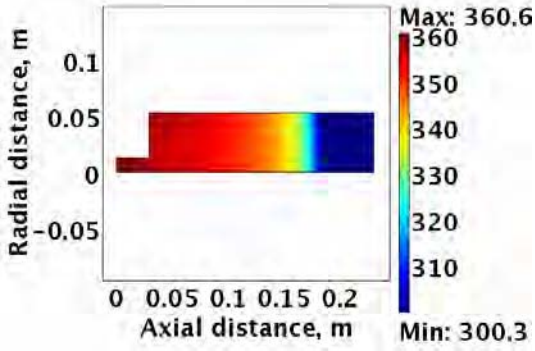

(b) 2 min

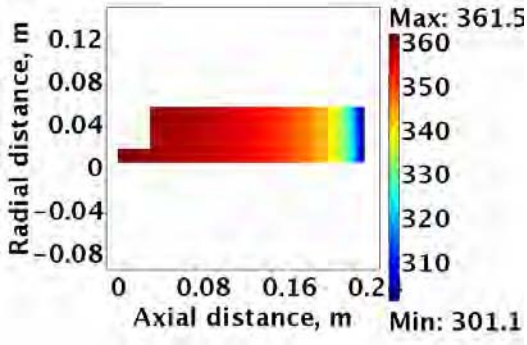

(c) 3 min

Figure 6. Temperature maps in the adsorbent bed at different times during charging of ANG cylinder at a flow rate of 30.0 *l* min^{-1}.

Table 2 Adsorption data at controlled flow rates

Q (l min^{-1})	ΔT_{max}	V_f (l)	$\frac{V_f}{V_{bed}}$ (V/V)	t_f (min)
1.0	21	120.0	65.9	120.0
30.0	58	99.0	54.4	3.3

5. Conclusion

This work has demonstrated the thermal behaviour of ANG storage system during dynamic charging conditions. At high charging rates (30.0 l min^{-1}), although filling time is about 3.3 min (within practically feasible range), the reduction of storage capacity of about 17.5% due to significant large temperature increase of about 58^0 compared to that of low charging rates (1.0 l min^{-1}) makes the system inefficient. The longer filling time of 2.0 hours with charging rate of 1.0 l min^{-1} also makes the system impractical.

The study illustrates that models such as those reported in this work can be used to optimize conditions for gas storage applications.

6. References

1. Basumatary, R., Dutta, P., Prasad, M. and Srinivasan, K., Thermal modeling of activated carbon based adsorptive natural gas storage system, *Carbon*, **43**, 541-549 (2005)

2. Chang, K.J. and Talu, O., Behaviour and performance of adsorptive natural gas storage cylinders during discharge, *Applied Thermal Engineering*, **16**, 359-374 (1996)

3. Goetz, V. and Biloe, S., Efficient dynamic charge and discharge of an adsorbed natural gas storage system, *Chem. Eng. Comm.*, **192**, 876-896 (2005)

4. Mota, J.P.B., Rodrigues, A.E., Saatdjian, E. and Tondeur, D., Dynamics of natural gas adsorption storage systems employing activated carbon, *Carbon*, **35**, 1259-1270 (1997)

5. Osawa, S., Kusumi, S. and Ogino, Y., Physical adsorption of gases at high pressure: an improvement of DA equation, *J. Colloidal Interface Sci.*, **56**, 83-91 (1976)

6. Ridha, F.N., Yunus, R.M., Rashid, M. and Ismail, A.F., Thermal transient behaviour of an ANG storage during dynamic discharge phase at room temperature, *Applied Thermal Engineering*, **27**, 55-62 (2007)

7. Stoeckli, F., Guillot, A., Slasli, A.M. and Hugi-Cleary, D., Pore size distributions of active carbons assessed by different techniques, *Carbon*, **38**, 929-941 (2000)

8. Vasiliev, L.L., Kanonchik, L.E., Mishkinis, D.A., and Rabetsky, M.I., Adsorbed natural gas storage and transportation vessels, *International Journal of Thermal Science*, **39**, 1047-1055 (2000)

7. Acknowledgements

The authors wish to acknowledge the financial support provided by BPCL, India, through project number 99131.

.